# Mechanical testing of antimicrobial biocomposite coating on metallic medical implants as drug delivery system

Karacan, Ipek; Ben-Nissan, Besim; Wang, Hang Andy; Juritza, Arion ; Swain, Michael; Mueller, Wolfgang; Chu, Joshua; Stamboulis, Artemis; Macha, Innocent; Taraschi, Valerio

*DOI:*
10.1016/j.msec.2019.109757



*Document Version*
Peer reviewed version

*Citation for published version (Harvard):*
Karacan, I, Ben-Nissan, B, Wang, HA, Juritza, A, Swain, M, Mueller, W, Chu, J, Stamboulis, A, Macha, I & Taraschi, V 2019, 'Mechanical testing of antimicrobial biocomposite coating on metallic medical implants as drug delivery system', *Materials Science and Engineering C*, vol. 104, 109757.
https://doi.org/10.1016/j.msec.2019.109757

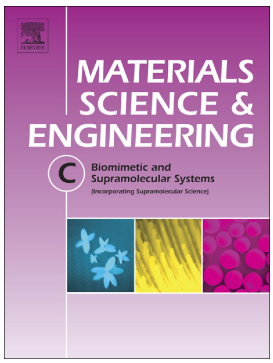


# Mechanical testing of antimicrobial biocomposite coating on metallic medical implants as drug delivery system

Ipek Karacan, Besim Ben-Nissan, Hang Andy Wang, Arion Juritza, Michael V. Swain, Wolfgang H. Müller, Joshua Chou, Artemis Stamboulis, Innocent J. Macha, Valerio Taraschi

PII: S0928-4931(19)30160-2
DOI: https://doi.org/10.1016/j.msec.2019.109757
Article Number: 109757
Reference: MSC 109757

To appear in: *Materials Science & Engineering C*

Received date: 14 January 2019
Revised date: 1 May 2019
Accepted date: 14 May 2019

Please cite this article as: I. Karacan, B. Ben-Nissan, H.A. Wang, et al., Mechanical testing of antimicrobial biocomposite coating on metallic medical implants as drug delivery system, Materials Science & Engineering C, https://doi.org/10.1016/j.msec.2019.109757

# Mechanical Testing of Antimicrobial Biocomposite Coating on Metallic Medical Implants as Drug Delivery System

Ipek Karacan[1], Besim Ben-Nissan[1], Hang Andy Wang[2], Arion Juritza[3], Michael V. Swain[2], Wolfgang H. Müller[3], Joshua Chou[1], Artemis Stamboulis[4], Innocent J. Macha[5], and Valerio Taraschi [1, 6]

[1] University of Technology Sydney, School of Life Sciences, NSW 2007, Sydney, Australia
[2] University of Sydney, NSW 2006, Sydney, Australia and Don State Technical University, Rostov-on Don, Russia

[3] Berlin University of Technology, Institute of Mechanics, LKM, Sekr. MS 2, Einsteinufer 5, 10587 Berlin, Germany

[4] University of Birmingham School of Metallurgy and Materials Edgbaston Birmingham B15 2TT, UK

[5] Department of Mechanical and Industrial Engineering, University of Dar es Salaam, P.O Box 35131, Tanzania.

[6] BresMedical Pty Ltd, 45 Lanacaster Street, Ingleburn NSW 2565 Australia

## Abstract

Post-operative infection often occurs following orthopedic and dental implant placement requiring systemic administered antibiotics. However, this does not provide long-term protection. Over the last few decades, alternative methods involving slow drug delivery systems based on biodegradable poly-lactic acid and antibiotic loaded hydroxyapatite microspheres were developed to prevent post-operative infection. In this study, thermally anodised and untreated Ti6Al4V discs were coated with poly-lactic acid (PLA) containing gentamicin (Gm) antibiotic-loaded coralline hydroxyapatite (HAp) are investigated. Following chemical characterization, mechanical properties of the coated samples were measured using nanoindentation and scratch tests to determine the elastic modulus, hardness and bonding adhesion between film and substrate. It was found that PLA biocomposite multilayered films were around 400nm thick and the influence and effect of the substrate were clearly observed during the nanoindentation studies with heavier loads. Scratch tests of PLA coated samples conducted at ~160nm depth showed minimal difference in the measured friction between Gm and non Gm containing films. It is also observed that the hardness values of PLA film coated anodised samples ranged from 0.45 to 1.9 GPa (dependent on the applied loads) against untreated coated samples which ranged from 0.28 to 0.8 GPa.

**Keywords:** Ti6Al4V-PLA-HAp biocomposite, hydroxyapatite, nanoindentation, scratch tests, thin films, nano-coating, antimicrobial.

## 1. Introduction

Titanium and titanium alloy metals are commonly used in orthopedic and maxillofacial implants and devices, due to their relatively low density, lower Young's modulus, high strength and corrosion resistance in comparison to other metallic biomaterials. During the last three decades it was found that TiAl4V alloy is the most attractive type of Ti alloy for the dental and orthopedic implant applications, because of its better mechanical properties [1-3]. Although Ti6Al4V alloy has high corrosion resistance, and biocompatibility properties, it has certain limitations, such as the release of Al and V ions, which may cause allergic reactions in certain patients with metal sensitivity [1, 2, 4]. On the other hand, although much better than any other metallic alloy, Young's modulus of Ti6Al4V (~110 GPa) is much higher than Young's modulus of human bone (~25 GPa) which might lead to complications in the long-term [3,5].

In order to improve the biological integration properties of metallic implants, various types of coating and surface modification methods have been proposed during the last fifty years [6]. According to the literature it is well accepted that surface modifications of the metallic implants can provide increased bioactivity and result in excellent osseointegration between the host tissue and the implant surface [6, 7].

In the early 1980s the introduction of plasma sprayed calcium phosphate coatings commenced that were used on both orthopedic and dental implants [8]. Later bioglass coatings and more recently nanocoatings were introduced. Surface micro-texturing to improve bone bonding was applied and is currently used on commercially available medical implants [8, 9, 10]. Research has shown that various additional surface treatment methods such as bone morphogenic proteins, collagen and recently stem cells were also beneficial for enhancing osseointegration. Novel nano thin film coatings, whose matrix materials consist of bioceramics such as calcium phosphates, and natural or synthetic polymers such as Poly Lactic Acid (PLA) have been proposed in some recent studies [11, 12].

Recently, Macha *et al.*, have shown that a new biocomposite coating material, consisting of both a bioceramic and a biodegradable polymer can be used for dental and orthopedic implants. These coatings on implants were designed to enable slow and targeted drug delivery systems to occur in order to inhibit post-operative complications arising from infection or to assist in drug delivery for cancer treatment [13, 14].

This new application has a drug delivery system based on a PLA thin film biocomposite which contains an antibiotic, Gentamicin (Gm), loaded into cHAp bioceramic microspheres (PLA-HAp-Gm). The hybrid consists of a PLA matrix (that might also contain Gm) and within coralline HAp microspheres of 100 nm diameter that have Gm loaded within its

pores. Coralline converted HAp structure contains both meso- and nano-pores in the bulk that can be easily loaded with antibiotics or other therapeutics and minerals [7, 8, 15, 16].

Macha *et al.* reported that a PLA-HAp-Gm film successfully prevents the growth of *Staphylococcus aureus*, which is one of the most important causes of bacterial infections after implant surgery. They also conducted dissolution studies on PLA thin film biocomposites and were able to adjust the coral to be either hydroxyapatite or tricalcium phosphate as well as to control the drug release rate [12, 13].

In recent research, surface morphology and structural characterization of Ti6Al4V alloy discs coated with PLA-HAp-Gm films by spin and dip coating methods were investigated [15].

The main aim of this current investigation is to determine the mechanical and the adhesion properties of these new generation hybrid coatings on titanium alloy.

## 2. Materials and Methods

### 2.1. Materials

The basic ingredients for this study included 2003D poly lactic acid (PLLA) (Nature Works, Ingeo Pty Ltd Australia) (MW; $2x10^4$ g/mol), porous coral skeleton samples (obtained from the Great Barrier Reef, QLD Australia with permission), as well as gentamicin sulfate, chloroform, sodium hypochlorite (NaClO) and diammonium hydrogen phosphate ($(NH_4)_2HPO_4$, 99%- Bio Ultra) (Sigma Aldrich, Castle Hill, Australia) and high purity Ti6Al4V rods and discs (Good Fellows UK).

### 2.2. Methods

In this new generation, implantable Ti6Al4V discs (∅ 20 mm) were coated with PLA biocomposites, which contained HAp microspheres as a drug carrier and Gm as the selected antibiotic.

In *Figure 1*, the process is shown schematically. In order to analyse the new drug delivery system, three different sets of samples were prepared, namely PLA, PLA-HAp, PLA-Gm and PLA-Gm-(HAp-Gm) coated Ti6Al4V. Two coating methods were used; spin and dip coating. *Spin* coating is more appropriate for flat surfaces, however, the dip coating method was chosen for this study, because it is readily applicable to both flat and complicated shapes of implants.

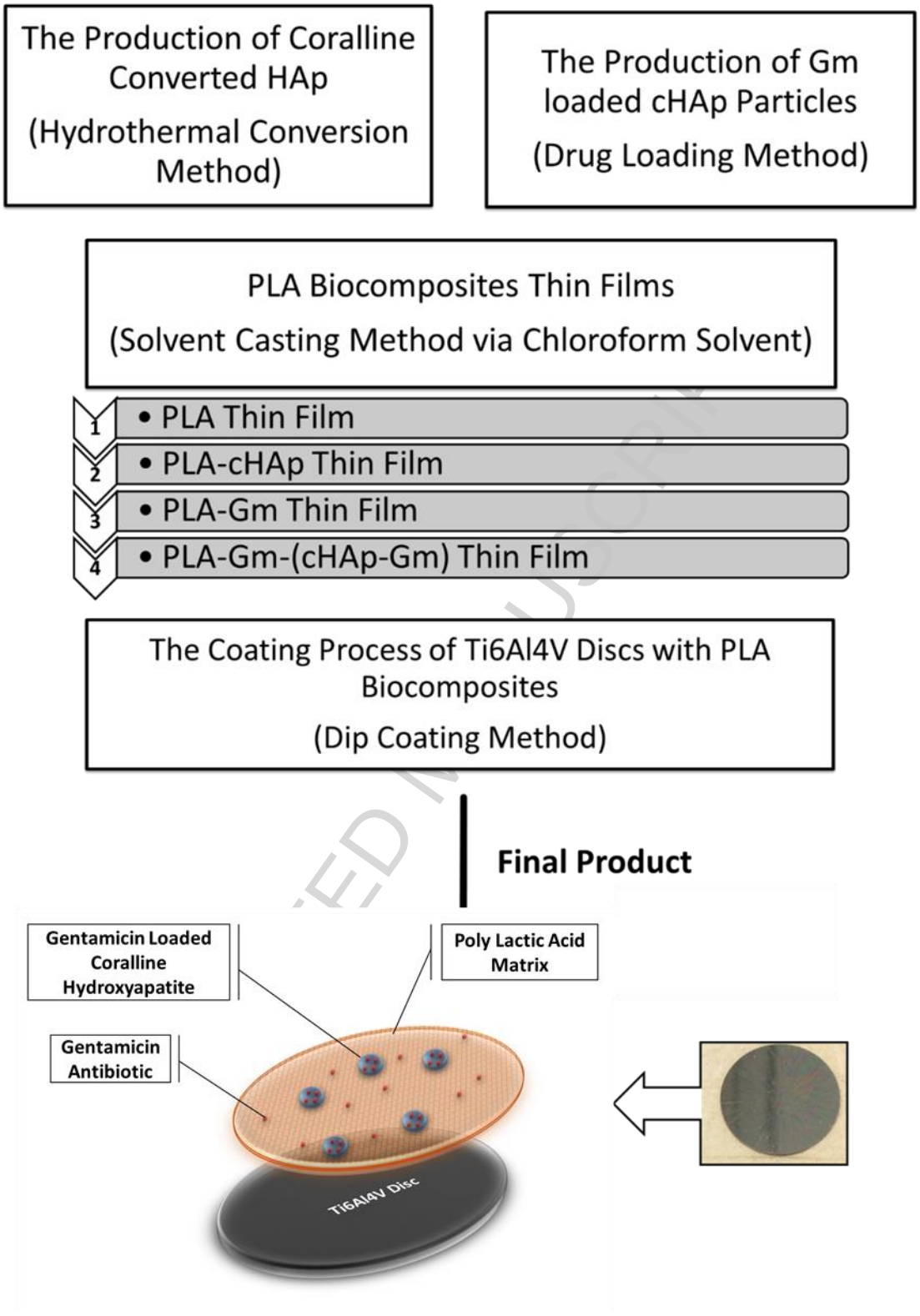


***Figure 1.*** Schematic representation of the production of PLA biocomposite films coated Ti6Al4V discs.

### 2.2.1. The Sample Preparation

**The Substrate Material Preparation**

Ti6Al4V discs were highly polished. First, the polishing was done with 320 grit, then by using 1200PSA silicon carbide papers. Final polishing was done with 0.2 μm alumina particles that were used in third and fourth steps in order to get a mirror surface. Ti6Al4V discs were cleaned with 100% acetone by ultra-sonication for 10min. They were dried under vacuum overnight within a desiccator.

Two sets of highly polished Ti6AL4V discs were prepared for this study. One set of samples were Ti6Al4V as is and the other set was anodised by thermal treatment. The thermal anodisation process was carried out at $500^0$C for 16 hours in air to obtain an oxidised layer on the surface of the discs.

**The Bioceramic Drug Carrier Material Preparation and Drug Loading Method**

The porous Porites coral, which is calcium carbonate and mostly aragonite, was converted to HAp microspheres in order to use as a drug carrier for the slow drug delivery system. Prior to conversion bulk coral pieces were ground by ball milling at 46 rpm overnight, after which the ground microspheres produced were cleaned with 2% (v/v) NaClO solution to assist with the removal of remnant organic matter. The final cleaned microspheres were converted to HAp via the hydrothermal conversion method at 220ºC and 160 Pa with $(NH_4)_2HPO_4$ as the phosphate conversion media, which aimed to achieve a Ca/P ratio of 1.67 [11, 16].

After HAp was obtained via the hydrothermal conversion method, a rotavaporator (Rotavaporator R-210) was used to load Gm antibiotic into the HAp microspheres. Drug loading was carried out with Rotary-evaporator at 60ºC and 100rpm based on previously published work [7]. The nano- and meso-porous structure of HAp particles were loaded with Gm antibiotic by dissolving the drug to the required amount in MilliQ water.

**The Synthesis of PLA Thin Films and the Coating Method**

PLA thin films designated as PLA, PLA-HAp, PLA-Gm, and PL-Gm-(HAp-Gm), respectively, were cast on a petri dish by the solvent casting technique using chloroform solvent as described previously [17]. PLA thin films were prepared by dissolving 0.5 g PLA particles into 30 mL chloroform solvent. Finally, the dip coating method was applied during which the discs were held by their edge and dipped into the HAp containing PLA solution at a constant speed [8]. After the coating process, all samples were placed in a vacuum furnace at 60 ºC for 16 hr. Each sample was coated four times to produce approximately a 400 nm multilayered biocomposite coating.

### 2.2.2. Characterization: surface structure and chemical composition

Specific surface area of coralline HAp was measured with a Tristar II apparatus from Micrometrics. Samples were initially degassed under vacuum at 77.3 K before analysis. The analysis was performed using the static method at -196.15$^{o}$C with nitrogen as the adsorbent. The Brunauer-Emmett-Teller (BET) method was applied to calculate the total surface area.

Surface structure, morphology and chemical composition of the PLA and PLA biocomposite coated discs were established by a Scanning Electron Microscope (SEM) (Zeiss Evo LS15) equipped with an EDX analyzer. The samples were sputter coated with a 7 nm thin layer of Au-Pd (Leica EM ACE600 Sputtering and Carbon Thread Coater) in order to reduce charging.

FT-IR spectra of the biocomposite coated samples were collected (Nicolet, Magna-IR 6700 Spectrometer FT-IR, Thermo-Scientific, Madison, USA), using the ATR mode, from wavenumber 2000 to 200 $cm^{-1}$ at a resolution of 4 $cm^{-1}$.

A profilometer (Dektak XT-stylus profiler) and an ellipsometer (JA Woollam Variable Angle Ellipsometer) were used to measure the thickness of the coated thin films.

### 2.2.3. Mechanical and Adhesion Testing

Nanoindentation of both treated (anodised) and untreated (un-anodised) Ti6Al4V substrates and the coated samples were carried out using a Nano-Triboindenter (Hysitron Inc., USA) with a calibrated Berkovich indenter for determination of hardness and elastic modulus while a < 1µm radius 90 included angle conical indenter tip was used for the scratch tests. All tests were conducted in ambient conditions. Two different load ranges were used with the Berkovich indenter in order to determine the properties accurately due to the film thickness and the influence of the indenter penetration depth.

Firstly, a range of 50-70mN loads was applied on treated (anodised) and untreated Ti6Al4V discs for both coated and uncoated forms to compare the effects of the treatment and PLA composite coating on the properties of the substrates. The loading rate ranged from 5 mN/s to 10 mN/s. Additionally, a maximum indentation depth of 1000 nm was used.

Secondly, a range of loads was applied which varied between 0.1 to 5 mN on all samples in order to determine mechanical properties of both coated and uncoated samples. The holding time at the maximum loads for all the tests was 20 s to minimize the time-dependent plastic creep deformation on the estimation of hardness and elastic modulus.

For the adhesion properties, a scratch tester (Hysitron Inc., USA) was used with a <1 µm conical indenter tip radius, and 160 µN load was applied. The speed of the scratch application was 0.25 µm/s, and the scratch length was 10 µm.

## 3. Results and Discussions

Anodised and untreated Ti6Al4V discs were successfully coated with PLA and PLA biocomposites containing HAp microspheres by dip coating method. The results show a very uniform and homogeneous coating, covering the surfaces of the samples. *Figure 2 (A-B)* shows highly polished anodised and untreated titanium samples before and after the PLA coating process respectively.

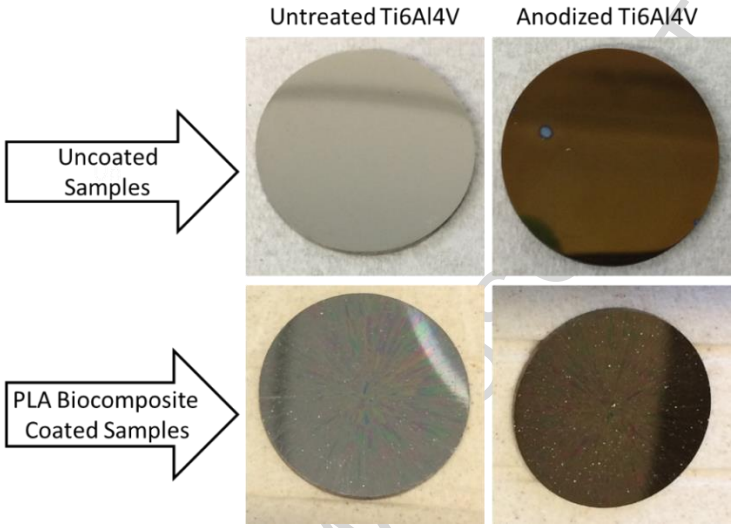


***Figure 2.*** The anodised and untreated Ti6Al4V discs before (A) and after (B) PLA biocomposite coating.

## 3.1. Characterization

The SEM observations of the surface morphology of both untreated and treated Ti6Al4V discs before coating are shown in *Figure 3*. While the untreated Ti6Al4V surface was observed to be smooth in *Figure 3*-A, the surface of anodised Ti6Al4V sample shows an "etch effect" associated with the oxide nanoparticles formed during the anodisation process (*Figure 3*-B).

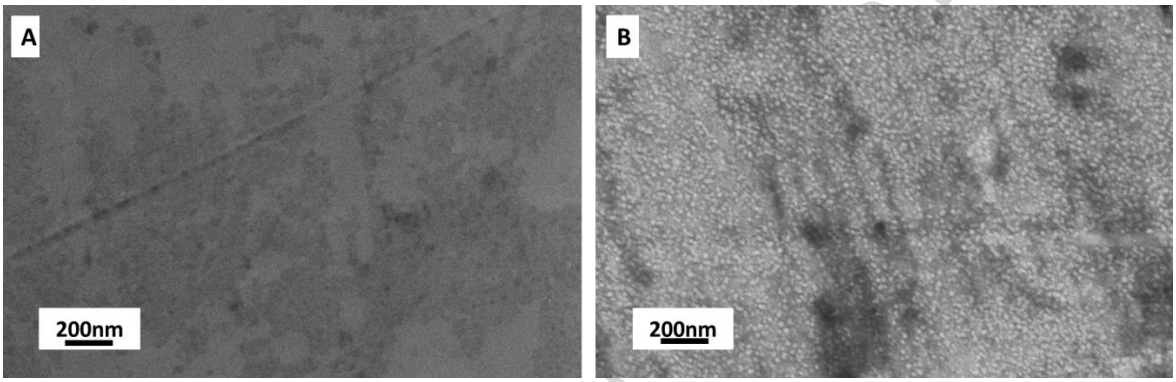


***Figure 3.*** SEM results of both uncoated [A] untreated and [B] anodised Ti6Al4V disc showing the surface structure differences before and after the anodisation process and the resultant grain structure on the treated Ti6Al4V disc.

The SEM results of the PLA biocomposite coating on Ti6Al4V discs are shown in *Figure 4* for both untreated and treated samples. The PLA coated sample (*Figure 4*-A) has a uniform surface with no surface or edge cracks. Although the PLA film is uniform on the surface of Ti6Al4V discs, a number of agglomerated particles were observed on the surfaces of the samples which are agglomerated Gm that has not mixed or being incorporated into the matrix (*Figure 4*-B, C, and D). Generally, Gm penetrates well after the rotovaporator loading and stays within the coralline apatite structure.

The only differences between *Figure 4* B-C and D (PLA-HAp, PLA-Gm, and PLA-Gm-(HAp-Gm) samples) were the extent of agglomerated and non-agglomerated particles and their size distribution. *Figure 4C*, however, shows the presence of undissolved Gm and agglomerated particles.

In order to determine the original particle size of HAp microspheres before the coating process, the Brunauer-Emmett-Teller (BET) testing method was used. The average particle size of HAp was 100 nm, and agglomerated particles up to 300-600 nm were measured, although in very small amounts, which corresponds to SEM observations (*Figure 4*D). Gm particles was mainly dissolved and deposited within the matrix and within the HAp particles although some agglomerated particles were also observed. Knowing that each microsphere of

HAp after ball milling was approximately 100 nm, it is quite reasonable that agglomeration produced the above-mentioned sizes.

For Gm loaded HAp containing composites, the HAp particles are spread more uniformly than for other PLA biocomposites.

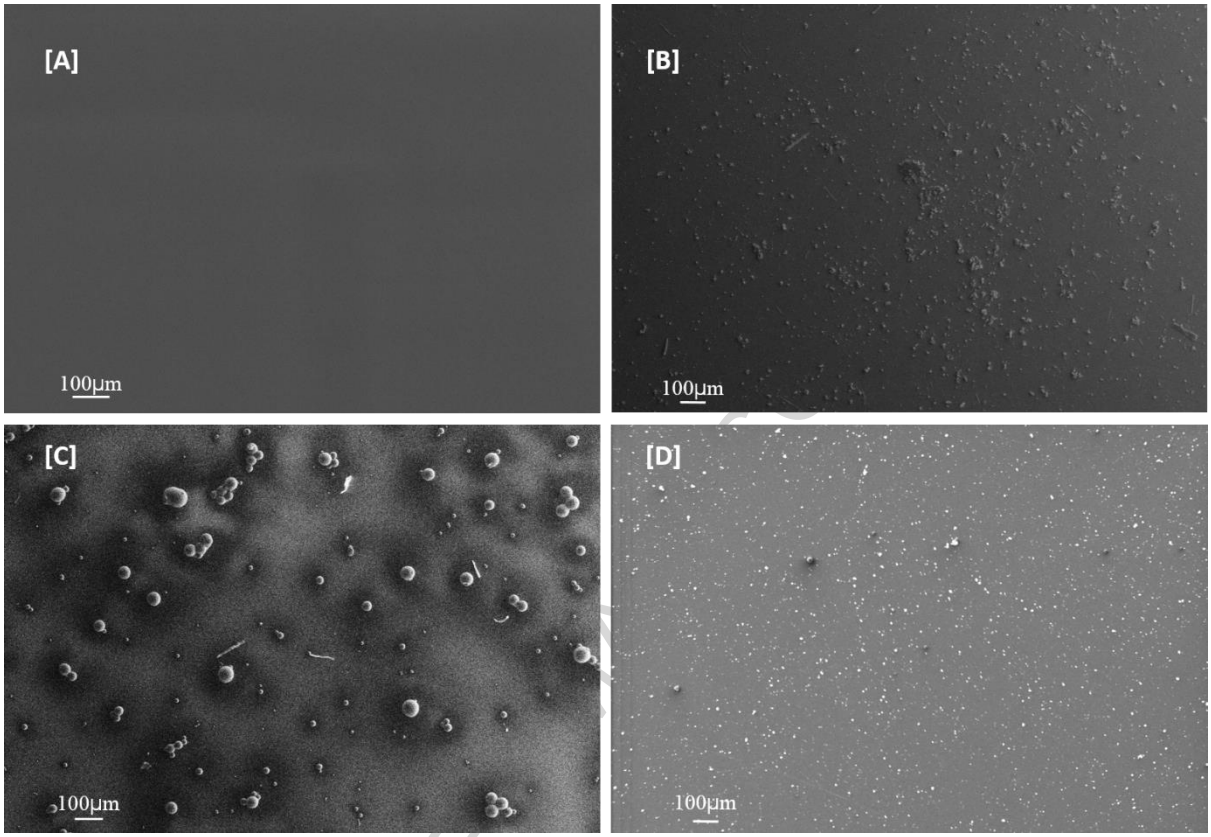


***Figure4.*** SEM results show the different PLA biocomposites matrix coated Ti6Al4V discs [A] only PLA which is smooth thin film coating, [B] PLA-HAp matrix coating with agglomerated HAp particles on the surface, [C], PLA-Gm coating with 10µm Gm particles on the surface, and [D] PLA-Gm-(HAp-Gm) biocomposite coating which is actual product with evenly distributed Gm- HAp particles on the surface.

Profilometry measurements show that the dip-coated samples have ~ 370nm film thicknesses. These results were also confirmed by the ellipsometer analysis.

FT-IR spectra results show for PLA thin film composites the following peaks: –C=O (1746 $cm^{-1}$), -C-H (1451-1358 $cm^{-1}$), -C-O ester (1180-1043 $cm^{-1}$) and -C-O stretch (867-751 $cm^{-1}$) in *Figure 5*-A. Additionally, the v4 $PO_4$ peaks (600-502 $cm^{-1}$) characteristic peaks of HAp were seen in Figure 5- B and D. Although HAp characteristic peaks are major peaks for PLA-HAp coated sample, they were minor peaks for PLA-Gm-(HAp-Gm) coated samples. The FT-IR spectra of PLA and HAp correctly match with literature values [18-20]. On the other hand, Gm characteristic peaks in Figure 4- C and D were obtained, as minor peaks, amide I-II

groups which are N-H stretch (1619 and 1523 $cm^{-1}$). This is in good agreement with the literature [21].

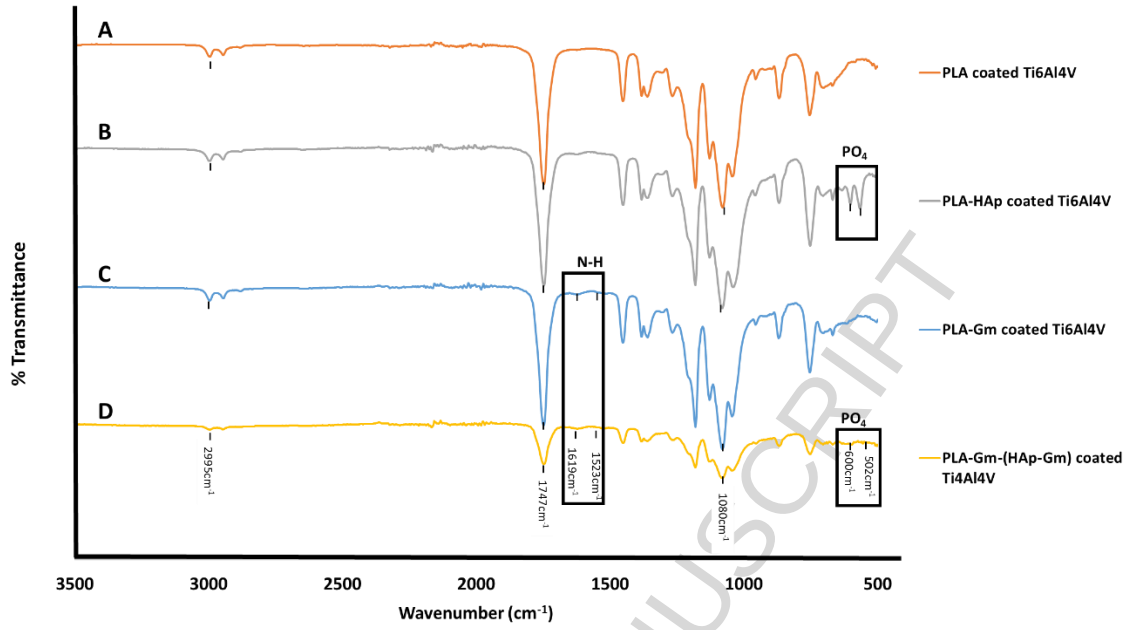


***Figure 5.*** FT-IR results of all sets of PLA biocomposite coated Ti6Al4V discs. The characteristic peaks of Gm (1619 and 1523 $cm^{-1}$ which are amide group I-II) and HAp (600-502 $cm^{-1}$ that are $PO_4$ group) were labeled on the spectrum separately.

## 3.2. The Analyses of the Mechanical and Adhesion Properties

Mechanical and adhesion properties of PLA films with and without HAp-Gm particles on the anodised and untreated Ti6Al4V discs were carried out using nanoindentation and scratch tests.

As shown in *Figure 6*, hardness (H) and modulus of elasticity (E) values of uncoated, anodised and untreated Ti6Al4V discs were obtained by nanoindentation analysis at high loads, namely 50-70 mN. The resultant indenter contact penetration depth ranged between 100 nm to 1000 nm in order to measure H and E values of both the surface oxidised layer and the Ti6Al4V substrate surface. Note that the H and E values of the oxidised layer, which were labeled on the figures, were higher than the untreated Ti6Al4V substrate.

*In Figure 6,* nanoindentation results of the anodised uncoated Ti6Al4V disc are shown, at low loads it can be clearly seen that the hardness values changes from 3.6 to 6.5 GPa, while the E values at low loads are between 90 to 120 GPa. Increased radius of indenter contact shows a marginal drop in H while elastic modulus shows a value closer to Ti6Al4V.On the other hand, for highly polished Ti6Al4V (untreated and uncoated) discs, *Figure 6* shows constant H and E values for both low and high contact radius.

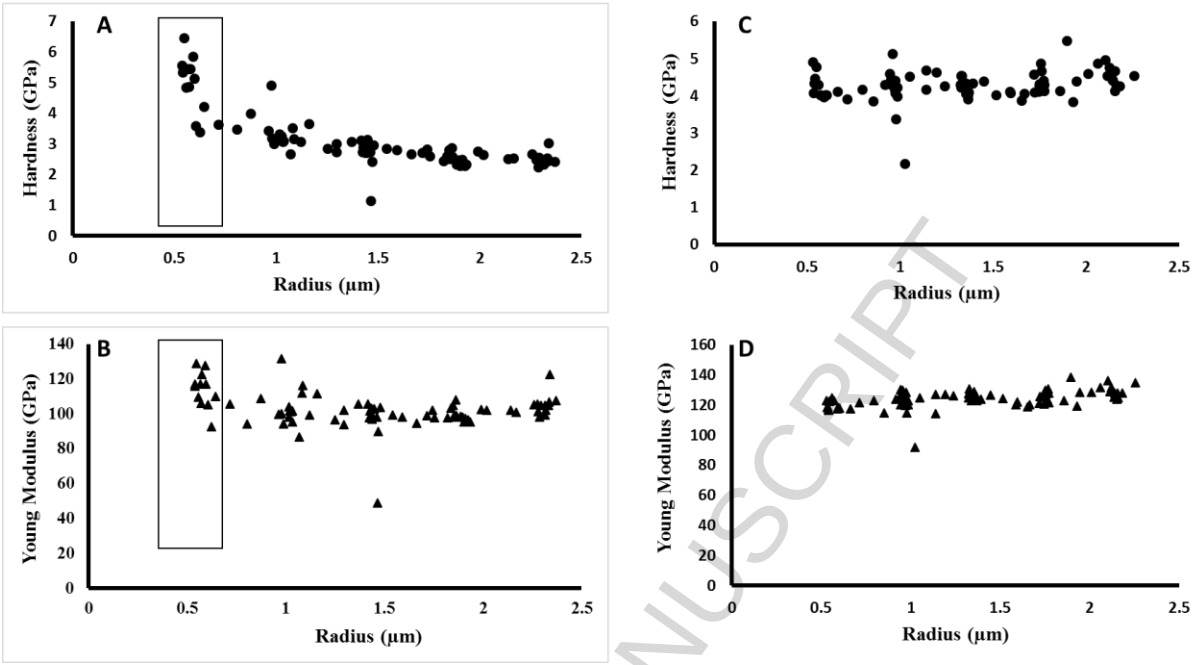


***Figure 6.*** Nanoindentation results for H and E plotted versus radius of contact at maximum load. (A) H and (B) E of treated uncoated Ti6Al4V disc respectively. (C) H and (D) E of untreated uncoated Ti6Al4V disc respectively. The influence of the anodised layers are labeled in both A and B graphs.

According to Figures 6-A and B, H and E values of the anodised uncoated Ti6Al4V sample at low loads were higher than untreated uncoated Ti6Al4V samples. Therefore, the nanoindentation analysis was conducted with low loads in order to compare anodised and untreated Ti6Al4V samples. The nanoindentation force-displacement curves in *Figure 7* show that the penetration depths for anodised Ti6Al4V samples were less and resulted in higher hardness and E modulus. These curves also show a major change of slope at approximately 50 nm penetration depth when the influence of the substrate occurs.

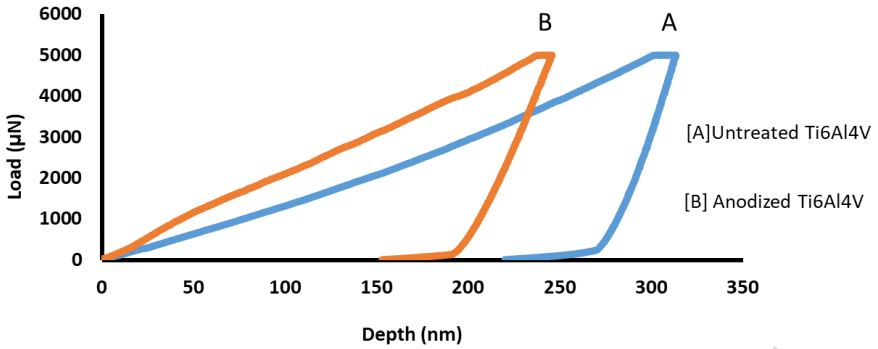


***Figure 7.*** Comparison of Berkovich force-displacement indentation observations of both uncoated [A] untreated and [B] anodised Ti6Al4V discs at 5mN load. Note the steeper initial slope and inflection of the curve for the anodised sample.

The influence of the anodisation process on the highly polished Ti6Al4V sample were observed during the application of the nanoindentation test on the anodised and untreated Ti6Al4V samples at high and low loads.

Afterward, PLA and PLA biocomposite coated anodised and untreated Ti6Al4V samples were analysed with the nanoindentation test at high and low loads, respectively, in order to observe the effects of anodisation process on the PLA matrix coating.

*Figure 8* shows the H and E values of anodised and untreated PLA-Gm-(HAp-Gm) coated Ti6Al4V discs, respectively. A PLA biocomposite coating effect on the anodised and untreated Ti6Al4V discs was seen in *Figure 8*. The H and E values were observed to range from around 0.5GPa to 2.0GPa, with the values increasing at higher loads.

During the nanoindentation tests a wide load range was used, which was between 50 and 70 mN. It was applied in order to compare results for a wide range of indentation depths. Because of the wide penetration depth difference between the indenter and the film thickness, the mechanical properties of PLA biocomposite films will be influenced by the substrate hardness (so called substrate effect) at high loads.

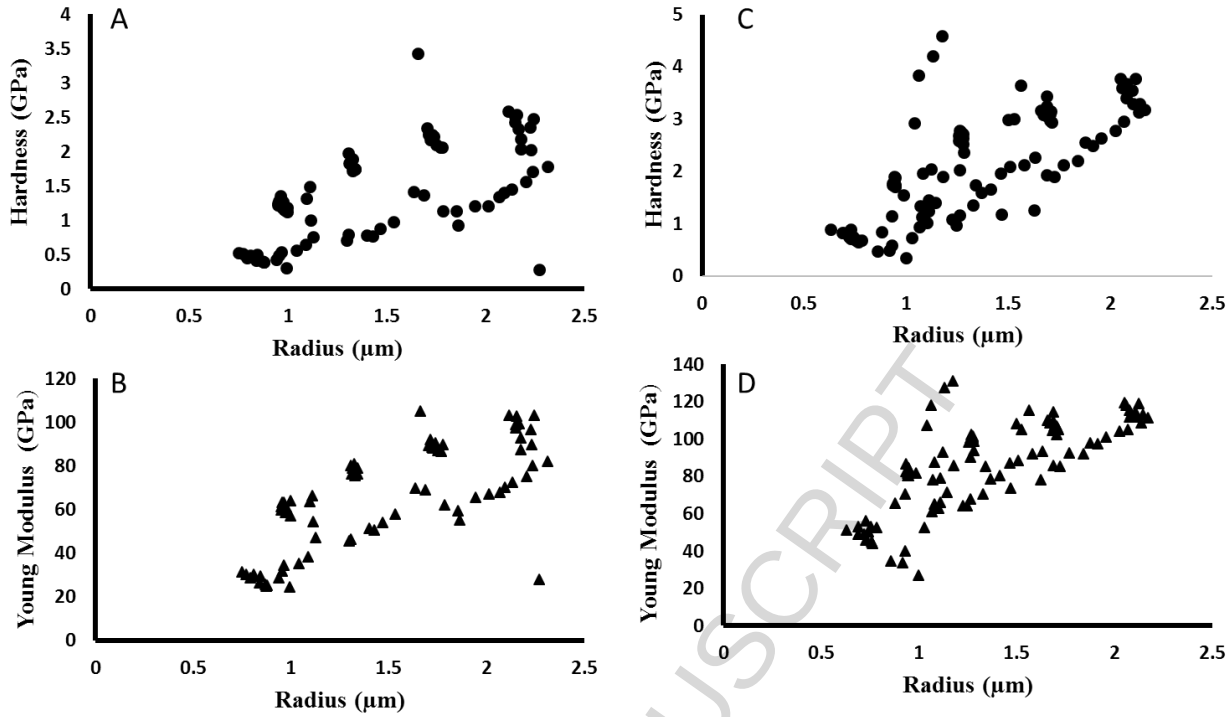


***Figure 8.*** Nanoindentation results of anodised PLA-Gm-(HAp-Gm) coated Ti6Al4V disc: (A) H values against Radius of contact, and (B) E values as a function of Radius, respectively; and nanoindentation results of untreated PLA-Gm-(HAp-Gm) coated Ti6Al4V disc: (C) H values versus contact radius, and (D) E values versus contact radius, respectively.

Nanoindentation results of PLA-Gm-(HAp-Gm) coated, anodised and untreated Ti6Al4V substrate surfaces are presented in *Figure 9* for low load range which is between 0.1 to 5 mN.

Applying low load is important to determine the mechanical properties of the coating materials without the influence of the substrate material. According to *Figure 9*, the penetration depth of PLA-Gm-(HAp-Gm) coated anodised and untreated samples can be observed clearly. For example, when 100μN load is applied on these two samples, the max penetration depth of anodised PLA-Gm-(HAp-Gm) sample is around 60nm, and untreated is around 120nm. Hence, the coated anodised samples produced harder coatings.

Similarly, nanoindentation of uncoated samples applied at low loads showed that force-displacement curves the penetration depth for anodised Ti6Al4V samples was less than untreated ones and hence higher hardness for anodised uncoated samples (*Figure 7).*

For the nanoindentation tests, at maximum loads, the maximum penetration depth was approx. 500 nm although the thickness of PLA film was only 375nm.

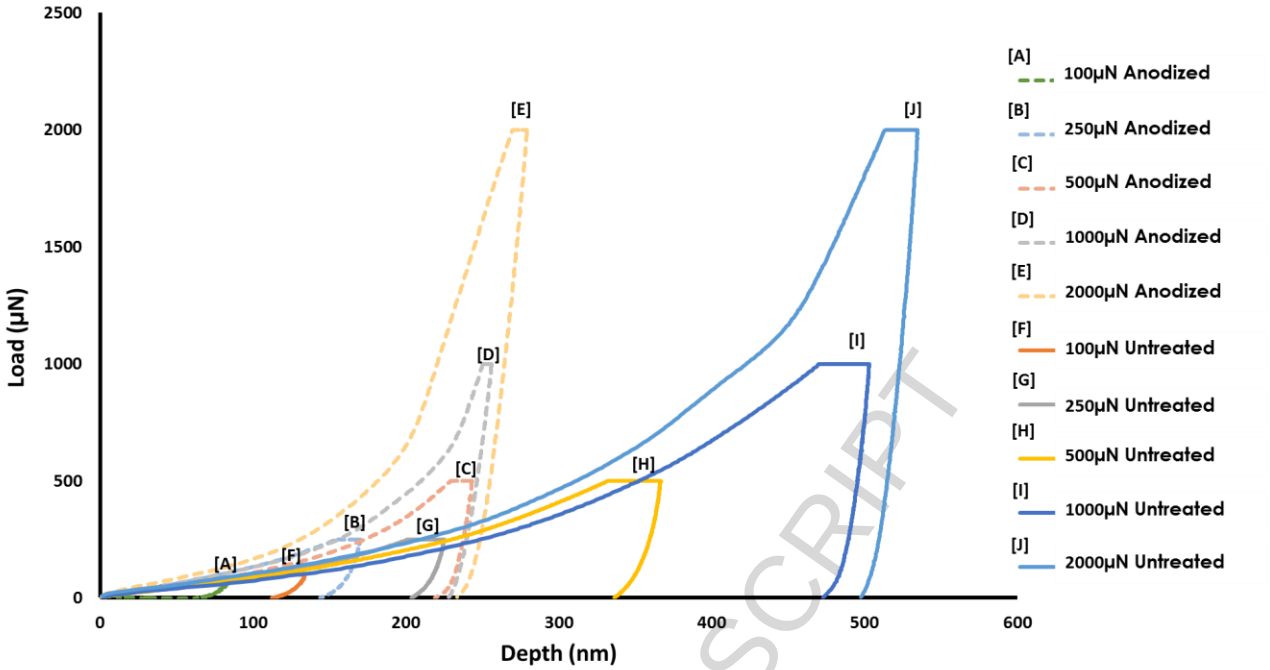


***Figure 9.*** Nanoindentation force-displacement observations of PLA-HAp-Gm coated anodised and untreated samples according to various loading conditions.

When the hardness and Young`s modulus versus penetration depth profiles of PLA-Gm-(HAp-Gm) anodised and untreated coated samples are compared, the anodised substrates show higher hardness and Young's modulus (E) values than untreated surfaces (*Figure 10)* for low load ranges (0.1-5mN).

Although the published values of Young's modulus of PLA bulk material is given as ~1.28 GPa [19], in *Figure 10*, it is seen that while E values for anodised PLA-Gm-(HAp-Gm) coated samples ranged between 20 to 70 GPa (dependent on applied loads). However for the untreated PLA-Gm-(HAp-Gm) coated samples it is between 20 to 50 GPa.

It is also observed that the hardness values of PLA film coated anodised samples ranged from 0.45 to 1.9 GPa (dependent on the applied loads) against untreated coated samples which ranged from 0.28 to 0.8 GPa, (*Figure 10)*. These results clearly show the substrate effect on the E and H values as a function of increased load.

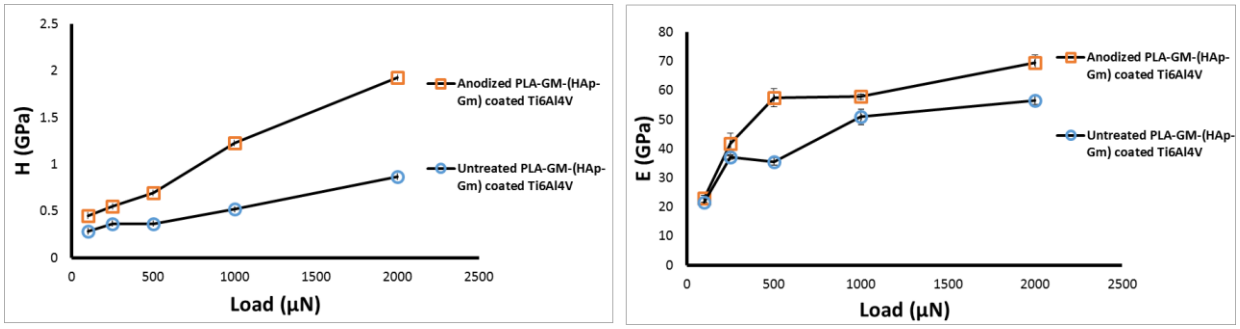


***Figure 10.*** Nanoindentation test results of E and H values of PLA-Gm-(HAp-Gm) coated anodised and untreated Ti6AL4V discs as a function of load.

In this study, scratch tests using a <1 µm conical tip radius, 160 µN constant low load and approximately 200nm indentation depth (which is smaller than the thickness of the film) were used in order to determine the frictional response and adhesion or bond strength of the films on Ti6Al4V samples. Plastic deformation is observed in all PLA biocomposite coated samples, which are shown in SPM results in *Figure 11*.

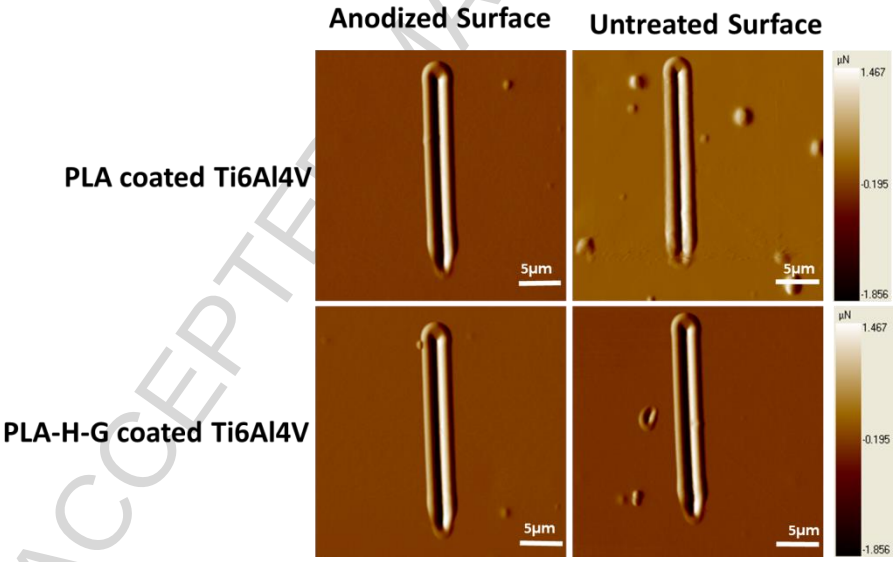


***Figure 11.*** Micro-scratch test results for anodised and untreated PLA biocomposite coated Ti6Al4V samples. These observations were generated by the SPM scan facility of the triboindenter system.

Plots of the coefficient of friction versus distance traveled are shown in *Figure 12* for all the samples. It was observed in *Figures 11* and *12* that when the PLA-Gm-(HAp-Gm) coating material is compared with only the PLA film, there was no indication of stick-slip like response nor evidence to suggest film delamination during scratching. Also, there are no statistically significant differences between their friction coefficient values. The presence of

the pile-up of material either side of the scratch indicates that plastic deformation is also observed on the PLA and PLA biocomposite coated surfaces with low loads as shown in Figure 8. The limited difference in appearance between the SPM scans for the anodised and untreated coated surfaces suggests that most of the deformation and pile-up occurred in the coating itself rather than the metallic substrate. An estimate of the contact pressure from the diameter of the track suggests that it is only ~16 to 20 MPa, well below the yield stress for deformation of the substrates.

For example, while untreated Ti6Al4V disc with PLA coating and untreated Ti6Al4V disc with PLA-Gm-(HAp-Gm) coating were compared, the friction coefficient value for untreated PLA coated sample is 0.680 ± 0.013, while the untreated PLA-Gm-(HAp-Gm) biocomposite coated sample is 0.658 ± 0.014.

The friction coefficient versus lateral displacement graphs were prepared in order to compare the parameters which influence the PLA biocomposite deposited on anodised and untreated Ti6Al4V surfaces (Figure 12).

Friction coefficient parameters are known to have two major contributions namely plowing and adhesion resistance forces [23]. The current observations suggest that while that the plastic ploughing contribution dominated the friction, the slight reductions in friction associated with the Gm containing films may be associated with a reduction in surface adhesion.

For anodised and untreated PLA, and PLA-Gm-(HAp-Gm) coated samples the resultant smooth tracks and the absence of stick-slip events during sliding indicate that both showed good adhesion to their respective substrates.

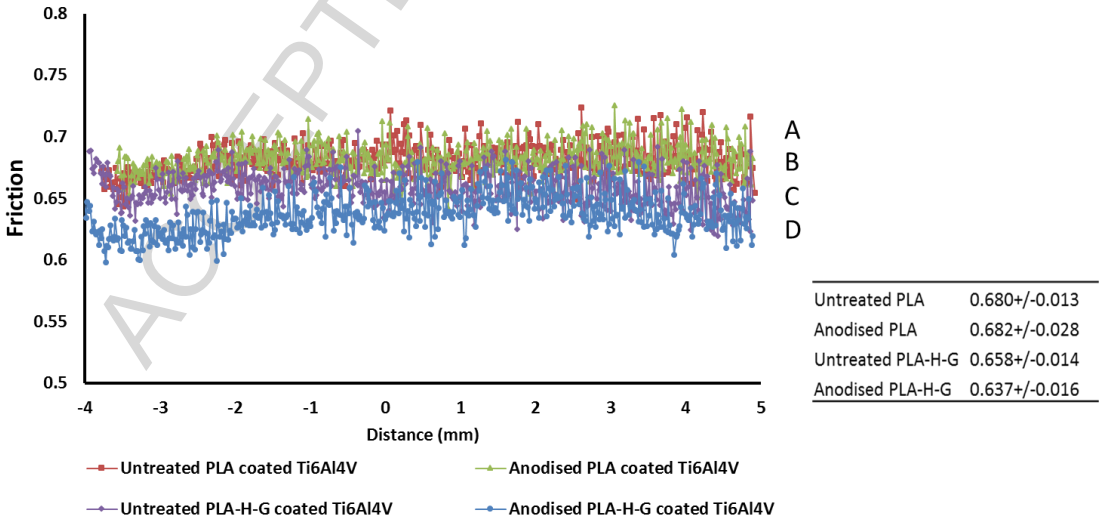


***Figure 12.*** Friction coefficient vs. Lateral displacement graph for [A] PLA coated untreated, [B] PLA coated anodised, [C] PLA-Gm-(HAp-Gm) coated untreated, [D] PLA-Gm-(HAp-Gm) coated anodised Ti6Al4V discs.

## 4. Conclusions

It can be concluded that:

1. The Ti6Al4V discs and implants can be successfully coated with multifunctional PLA biocomposites.
2. SEM results show that, PLA-Gm-(HAp-Gm) coated Ti6Al4V samples have uniformly distributed Gm within the composite.
3. FT-IR, XRD and SEM showed clearly that Gm is within the matrix and the hydroxyapatite particles and it is strongly bonded to particles and the matrix.
4. The nanoindentation results for uncoated but for treated and untreated Ti6Al4V discs at both high and low loads showed that both H and E values of the treated Ti6Al4V are higher than that untreated Ti6Al4V samples which ranged between 0.1 to 5 mN.
5. PLA-Gm-(HAp-Gm) coated treated samples showed E values of 20 to 70 GPa and H values of 0.45 to 1.9 GPa. However, for untreated samples E values ranged from 20 to 50 GPa and H values from 0.28 to 0.8 GPa
6. Nanoindentation studies clearly confirm that the increased E and H values observed at different applied loads are due to the substrate effect which is dependent on the indenter penetration depth, applied load value and the thickness of the films.
7. In PLA coated biocomposites the polymeric matrix H decreased in a range from 3-4GPa to 0.28-0.8GPa and E from 120-140GPa to 20-50GPa for both treated and also untreated samples.
8. The scratch test results showed that the insertion of HAp and Gm particles into the PLA thin films does not influence the friction coefficient.
9. The results of nanoindentation clearly support the results of the scratch tests at low loads, and they show that the PLA film coated treated samples are harder than PLA untreated samples.
10. For realistic H and E results with both scratch and nanoindentation tests low loads should be utilised with indenter penetration less than the film thickness.

## Acknowledgements

The authors would like to acknowledge and thank the Australian Academy of Science, and the European Commission “Horizon 2020” grants for their financial support.

## References

[1] A. Cigada, M. Cabrini, P. Pedeferri, Increasing of the corrosion resistance of the Ti6Al4V alloy by high thickness anodic oxidation, J. Mater. Sci. Mater. Med. 3 (1992) 408–412. doi:10.1007/BF00701236.

[2] D. Nowak, B. Januszewicz, P. Niedzielski, Morphology, mechanical and tribological properties of hybrid carbon layer fabricated by Radio Frequency Plasma Assisted Chemical Vapor Deposition, Surf. Coatings Technol. 329 (2017) 1–10. doi:10.1016/j.surfcoat.2017.09.001.

[3] A. Ataee, Y. Li, D. Fraser, G. Song, C. Wen, Anisotropic Ti-6Al-4V gyroid scaffolds manufactured by electron beam melting (EBM) for bone implant applications, Mater.

Des. 137 (2018) 345–354. doi:10.1016/j.matdes.2017.10.040.

[4] P. Rath, L. Besra, B. Singh, Titania/hydroxyapatite bi-layer coating on Ti metal by electrophoretic deposition: Characterization and corrosion studies, Ceramics International, 38 (2012) 3209-3216. doi: 10.1016/j.ceramint.2011.12.026

[5] F. Guillemot, Recent advances in the design of titanium alloys for orthopedic applications, Expert Rev. Med. Devices. 2 (2005) 741–748. doi:10.1586/17434440.2.6.741.

[6] B. Ben-Nissan, I.J. Macha, S. Cazalbou, A.H. Choi, Calcium phosphate nanocoatings and nanocomposites, part 2: thin films for slow drug delivery and osteomyelitis, Nanomedicine. 11 (2016) 531–544. doi:10.2217/nnm.15.220.

[7] R. Roest, B.A. Latella, G. Heness, B. Ben-Nissan, Adhesion of sol-gel derived hydroxyapatite nanocoatings on anodised pure titanium and titanium (Ti6Al4V) alloy substrates, Surf. Coatings Technol. 205 (2011) 3520–3529. doi:10.1016/j.surfcoat.2010.12.030.

[8] B. Ben-Nissan, A.H. Choi, A. Bendavid, Mechanical properties of inorganic biomedical thin films and their corresponding testing methods, Surface & Coating Technologhy, 233 (2013) 39-48.

[9] B-Ben-Nissan, A.H. Choi, Nanobioceramics for Healthcare Applications, Chapter5 Calcium Phosphate Nanocoatings : Production , Physical and Biological Properties , and Biomedical Applications, (2016) 105-150.

[10] I.J. Macha, B. Ben-Nissan, B. Milthorpe, Improvement of elongation in nanosurface modified bioglass/PLA thin film composites, Curr. Nanosci. 10 (2014) 200–204. doi:10.2174/15734137096661311290006 43.

[11] A.J.R. Lasprilla, A.G.R. Martinez, B.H. Lunelli, J.E.J. Figueroa, A.L. Jardini, R.M. Filho, Synthesis and Characterization of Poly ( Lactic Acid ) for Use in Biomedical Field, Chem. Eng. Trans. 24 (2010) 985–990. doi:10.3303/CET1124165.

[12] S. Farah, D.G. Anderson, R. Langer, Physical and mechanical properties of PLA, and their functions in widespread applications — A comprehensive review, Adv. Drug Deliv. Rev. 107 (2016) 367–392. doi:10.1016/j.addr.2016.06.012.

[13] L. Nikolic, I. Ristic, B. Adnadjevic, V. Nikolic, J. Jovanovic, M. Stankovic, Novel Microwave-Assisted Synthesis of Poly(D,L-lactide): The Influence of Monomer/Initiator Molar Ratio on the Product Properties, Sensors. 10 (2010) 5063–5073. doi:10.3390/s100505063.

[14] B.C. Cope, D.E. Packham, G. Leggett, J.C. Beech, G.B. Lowe, D. Briggs, D.M. Brewis, A.D. Crocombe, D.G. Dixon, W.J. Van Ooij, B. Parbhoo, C.M. Warwick, J. Pritchard, S. Millington, C. Chatfield, J. Comyn, D.A. Dillard, B. Kneafsey, M.E.R. Shanahan, A. V Pocius, Scratch Test, in: Handb. Adhes., John Wiley & Sons, Ltd, Chichester, UK, 2005: pp. 439–525. doi:10.1002/0470014229.ch17.

[15] I. Karacan, I.J. Macha, G. Choi, S. Cazalbou, B. Ben-Nissan, Antibiotic Containing Poly Lactic Acid/Hydroxyapatite Biocomposite Coatings for Dental Implant Applications, Key Eng. Mater. 758 (2017) 120–125. doi:10.4028/www.scientific.net/KEM.758.120.

[16] B. Ben-Nissan, Natural bioceramics: From coral to bone and beyond, Curr. Opin. Solid State Mater. Sci. 7 (2003) 283–288. doi:10.1016/j.cossms.2003.10.001.

[17] R. Roest, B.A. Latella, G. Heness, B. Ben-Nissan, Adhesion of sol-gel derived hydroxyapatite nanocoatings on anodised pure titanium and titanium (Ti6Al4V) alloy substrates, Surf. Coatings Technol. 205 (2011) 3520–3529. doi:10.1016/j.surfcoat.2010.12.030.

[18] A.J.R. Lasprilla, A.G.R. Martinez, B.H. Lunelli, J.E.J. Figueroa, A.L. Jardini, R.M. Filho, Synthesis and Characterization of Poly ( Lactic Acid ) for Use in Biomedical Field, Chem. Eng. Trans. 24 (2010) 985–990. doi:10.3303/CET1124165.

[19] S. Farah, D.G. Anderson, R. Langer, Physical and mechanical properties of PLA, and their functions in widespread applications — A comprehensive review, Adv. Drug Deliv. Rev. 107 (2016) 367–392. doi:10.1016/j.addr.2016.06.012.

[20] L. Nikolic, I. Ristic, B. Adnadjevic, V. Nikolic, J. Jovanovic, M. Stankovic, Novel Microwave-Assisted Synthesis of Poly(D,L-lactide): The Influence of Monomer/Initiator Molar Ratio on the Product Properties, Sensors. 10 (2010) 5063–5073. doi:10.3390/s100505063.

[21] A. Sionkowska, B. Kaczmarek, R. Gadzala-Kopciuch, Gentamicin release from chitosan and collagen composites, 35 (2016) 353-359.

[22] B.C. Cope, D.E. Packham, G. Leggett, J.C. Beech, G.B. Lowe, D. Briggs, D.M. Brewis, A.D. Crocombe, D.G. Dixon, W.J. Van Ooij, B. Parbhoo, C.M. Warwick, J. Pritchard, S. Millington, C. Chatfield, J. Comyn, D.A. Dillard, B. Kneafsey, M.E.R. Shanahan, A. V Pocius, Scratch Test, in: Handb. Adhes., John Wiley & Sons, Ltd, Chichester, UK, 2005: pp. 439–525. doi:10.1002/0470014229.ch17.

[23] J. Ballarre, E. Jimenez-Pique, M. Anglada, S.A. Pellice, A.L. Cavalieri, Mechanical characterization of nano-reinforced silica based sol–gel hybrid coatings on AISI 316L stainless steel using nanoindentation techniques, Surf. Coatings Technol. 203 (2009) 3325–3331. doi:10.1016/j.surfcoat.2009.04.014.

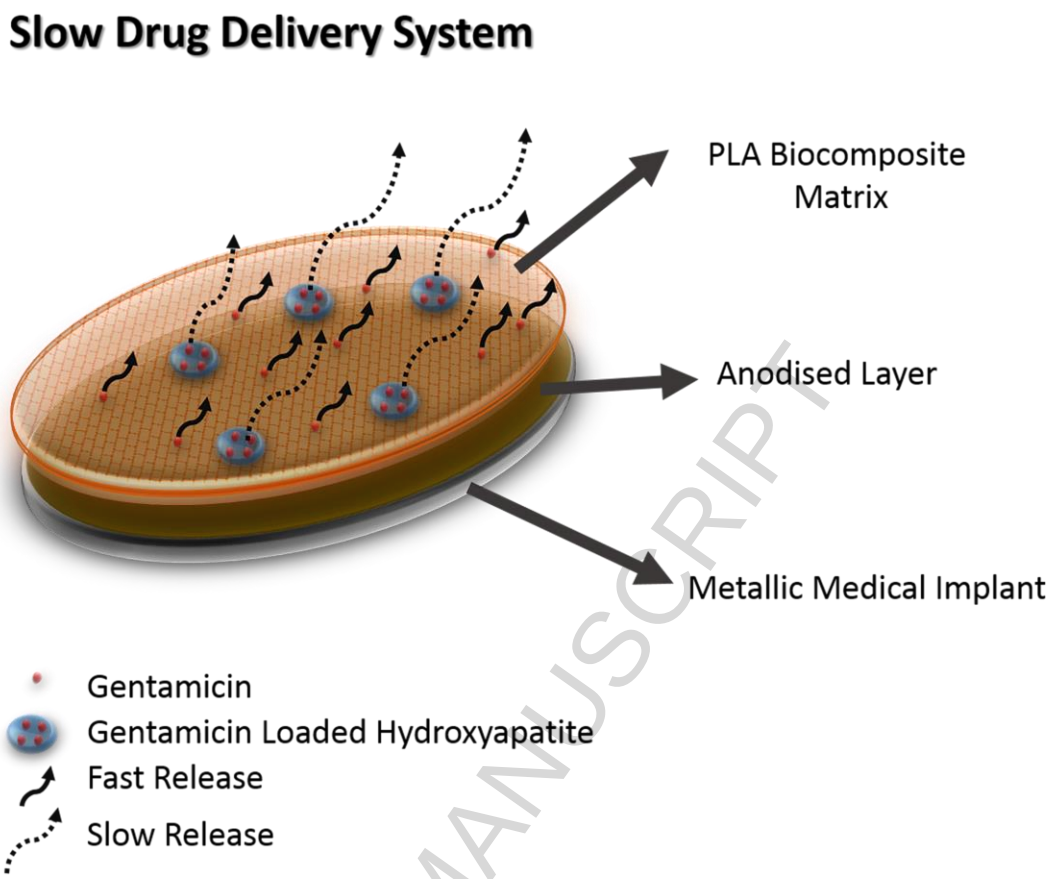


Graphical abstract